

A 125 GeV Higgs and its di-photon signal in different SUSY models: a mini review

Zhaoxia Heng

Department of Physics, Henan Normal University, Xinxiang 453007, China

Abstract

In this note we briefly review our recent studies on a 125 GeV Higgs and its di-photon signal rate in different low energy supersymmetric models, namely the minimal supersymmetric standard model (MSSM), the next-to-minimal supersymmetric standard model (NMSSM), the nearly minimal supersymmetric standard model (nMSSM) and the constrained MSSM. Our conclusion is: (i) In the allowed parameter space the SM-like Higgs boson can easily be 125 GeV in the MSSM, NMSSM and nMSSM, while it is hard to realize in the constrained MSSM; (ii) The di-photon Higgs signal rate in the nMSSM and constrained MSSM is suppressed relative to the prediction of the SM, while the signal rate can be enhanced in the MSSM and NMSSM; (iii) The NMSSM may allow for a lighter top-squark than the MSSM, which can thus ameliorate the fine-tuning problem.

PACS numbers:

I. INTRODUCTION

Considering the important role of the Higgs boson in particle physics, hunting for it has been one of the major tasks of the running Large Hadron Collider (LHC). Recently, both the ATLAS and CMS collaborations have reported some evidence for a light Higgs boson near 125 GeV [1, 2] with a di-photon signal rate slightly above the SM prediction [3].

As is well known, in new physics beyond the SM model several Higgs bosons are predicted, among which the SM-like one may be near 125 GeV [4–7]. Recently, in our studies [6, 7] we examined the mass of the SM-like Higgs boson in several supersymmetric (SUSY) models including the minimal supersymmetric standard model (MSSM)[8, 9], the next-to-minimal supersymmetric standard model (NMSSM)[10, 11] and the constrained MSSM[12, 13]. At tree-level, these SUSY models are hard to predict a Higgs boson near 125 GeV, and sizable radiative corrections, which mainly come from the top and top-squark loops, are necessary to enhance the Higgs boson mass[14]. Due to the different properties of these SUSY models, the loop contributions to the Higgs boson mass are different for giving a 125 GeV Higgs boson. Therefore, different models have different lower bounds on the top-squark mass which is associated with the fine-tuning problem [15]. On the other hand, since the di-photon Higgs signal is the most promising discovery channel for a light Higgs boson at the LHC[16], in our recent study [17] we performed a comparative study for the di-photon Higgs signal in different SUSY models, namely the MSSM, NMSSM and the nearly minimal supersymmetric standard model (nMSSM) [18, 19]. In this note we briefly review these studies on a 125 GeV Higgs boson and its di-photon signal rate in different SUSY models.

This note is organized as follows. In the next section we briefly describe the Higgs sector and the di-photon Higgs signal in these SUSY models. Then we present the numerical results and discussions in Sec. III. Finally, the conclusions are given in Sec. IV.

II. THE HIGGS SECTOR AND DI-PHOTON SIGNAL RATE IN SUSY MODELS

A. The Higgs sector in SUSY models

Different from the SM, the Higgs sector in the supersymmetric models is usually extended by adding Higgs doublets and/or singlets. The most economical realization is the MSSM, which consists of two Higgs doublet H_u and H_d . In order to solve the μ -problem and

the little hierarchy problem in the MSSM, the singlet extension of MSSM, such as the NMSSM[10] and nMSSM[18, 19] has been intensively studied[20]. The differences between these models come from their superpotentials and the corresponding soft-breaking terms, which are given by:

$$W_{\text{MSSM}} = W_F + \mu \hat{H}_u \cdot \hat{H}_d, \quad (1)$$

$$W_{\text{NMSSM}} = W_F + \lambda \hat{H}_u \cdot \hat{H}_d \hat{S} + \frac{1}{3} \kappa \hat{S}^3, \quad (2)$$

$$W_{\text{nMSSM}} = W_F + \lambda \hat{H}_u \cdot \hat{H}_d \hat{S} + \xi_F M_n^2 \hat{S}, \quad (3)$$

$$V_{\text{soft}}^{\text{MSSM}} = \tilde{m}_u^2 |H_u|^2 + \tilde{m}_d^2 |H_d|^2 + (B\mu H_u \cdot H_d + h.c.), \quad (4)$$

$$V_{\text{soft}}^{\text{NMSSM}} = \tilde{m}_u^2 |H_u|^2 + \tilde{m}_d^2 |H_d|^2 + \tilde{m}_S^2 |S|^2 + (A_\lambda \lambda S H_u \cdot H_d + \frac{A_\kappa}{3} \kappa S^3 + h.c.), \quad (5)$$

$$V_{\text{soft}}^{\text{nMSSM}} = \tilde{m}_u^2 |H_u|^2 + \tilde{m}_d^2 |H_d|^2 + \tilde{m}_S^2 |S|^2 + (A_\lambda \lambda S H_u \cdot H_d + \xi_S M_n^3 S + h.c.), \quad (6)$$

where W_F is the MSSM superpotential without the μ term, λ , κ and ξ_F are the dimensionless parameters and \tilde{m}_u , \tilde{m}_d , \tilde{m}_S , B , A_λ , A_κ and $\xi_S M_n^3$ are soft-breaking parameters. Note that in the NMSSM and nMSSM the μ -term is replaced by the $\mu_{\text{eff}} = \lambda s$ when the singlet Higgs field \hat{S} develops a VEV s . The differences between the NMSSM and nMSSM reflect the last term in the superpotential, where the cubic singlet term $\kappa \hat{S}^3$ in the NMSSM is replaced by a tadpole term $\xi_F M_n^2 \hat{S}$ in the nMSSM. This replacement in the superpotential makes the nMSSM has no discrete symmetry and thus free of the domain wall problem that the NMSSM suffers from. Actually, due to the tadpole term $\xi_F M_n^2$ does not induce any interaction, the nMSSM is identical to the NMSSM with $\kappa = 0$, except for the minimization conditions of the Higgs potential and the tree-level Higgs mass matrices.

With the superpotentials and the soft-breaking terms giving above, one can get the Higgs potentials of these SUSY models, and then can derive the Higgs mass matrices and eigenstates. At the minimum of the potential, the Higgs fields H_u , H_d and S are expanded as

$$H_u = \begin{pmatrix} H_u^+ \\ v_u + \frac{\phi_u + i\varphi_u}{\sqrt{2}} \end{pmatrix}, \quad H_d = \begin{pmatrix} v_d + \frac{\phi_d + i\varphi_d}{\sqrt{2}} \\ H_d^- \end{pmatrix}, \quad S = s + \frac{1}{\sqrt{2}} (\sigma + i\xi), \quad (7)$$

with $v = \sqrt{v_u^2 + v_d^2} = 174$ GeV. By unitary rotation the mass eigenstates can be given by

$$\begin{pmatrix} h_1 \\ h_2 \\ h_3 \end{pmatrix} = S \begin{pmatrix} \phi_u \\ \phi_d \\ \sigma \end{pmatrix}, \quad \begin{pmatrix} a \\ A \\ G^0 \end{pmatrix} = P \begin{pmatrix} \varphi_u \\ \varphi_d \\ \xi \end{pmatrix}, \quad \begin{pmatrix} H^+ \\ G^+ \end{pmatrix} = U \begin{pmatrix} H_u^+ \\ H_d^+ \end{pmatrix}. \quad (8)$$

where h_1, h_2, h_3 are physical CP-even Higgs bosons ($m_{h_1} < m_{h_2} < m_{h_3}$), a, A are CP-odd Higgs bosons, H^\pm is the charged Higgs boson, and G^0, G^\pm are Goldstone bosons eaten by Z and W^\pm . Due to the absence of the singlet field S , the MSSM only has two CP-even Higgs bosons and one CP-odd Higgs bosons, as well as one pair of charged Higgs bosons.

At the tree-level, the Higgs masses in the MSSM are conventionally parameterized in terms of the mass of the CP-odd Higgs boson (m_A) and $\tan \beta \equiv v_u/v_d$ and the loop corrections typically come from top and stop loops due to their large Yukawa coupling. For small splitting between the stop masses, an approximate formula of the lightest Higgs boson mass is given by[23],

$$m_h^2 \simeq M_Z^2 \cos^2 2\beta + \frac{3m_t^4}{4\pi^2 v^2} \ln \frac{M_S^2}{m_t^2} + \frac{3m_t^4}{4\pi^2 v^2} \frac{X_t^2}{M_S^2} \left(1 - \frac{X_t^2}{12M_S^2} \right), \quad (9)$$

where $M_S = \sqrt{\tilde{m}_{\tilde{t}_1} \tilde{m}_{\tilde{t}_2}}$ and $X_t \equiv A_t - \mu \cot \beta$. The formula manifests that larger M_S or $\tan \beta$ is necessary to push up the Higgs boson mass. And the Higgs boson mass can reach a maximum when $X_t/M_S = \sqrt{6}$ for given M_S (i.e. the so-called m_h^{max} scenario). Note that the lightest Higgs boson is the SM-like Higgs boson h (with the largest coupling to vector bosons) in most of the MSSM parameter space.

Different from the case in the MSSM, the Higgs sector in the NMSSM depends on the following six parameters,

$$\lambda, \quad \kappa, \quad M_A^2 = \frac{2\mu(A_\lambda + \kappa s)}{\sin 2\beta}, \quad A_\kappa, \quad \tan \beta = \frac{v_u}{v_d}, \quad \mu = \lambda s. \quad (10)$$

and in the nMSSM the input parameters in the Higgs sector are

$$\lambda, \quad \tan \beta, \quad \mu, \quad A_\lambda, \quad \tilde{m}_S, \quad M_A^2 = \frac{2(\mu A_\lambda + \lambda \xi_F M_n^2)}{\sin 2\beta}. \quad (11)$$

Because the coupling $\lambda \hat{H}_u \cdot \hat{H}_d \hat{S}$ in the superpotential, the tree-level Higgs boson mass has an additional contribution in the NMSSM and nMSSM,

$$\Delta m_h^2 = \lambda^2 v^2 \sin^2 2\beta \quad (12)$$

In order to push up the tree-level Higgs boson mass, λ has to be as large as possible and $\tan \beta$ has to be small. The requirement of the absence of a Landau singularity below the GUT scale implies that $\lambda \lesssim 0.7$ at the weak scale, and the upper bound on λ at the weak scale depends strongly on $\tan \beta$ and grows with increasing $\tan \beta$ [24]. However, this can still lead to a larger tree-level Higgs boson mass than in the MSSM. Therefore, the radiative

corrections to m_h^2 may be reduced in the NMSSM and nMSSM, which may induce light top-squark and ameliorate the fine-tuning problem[21].

In the NMSSM and nMSSM, due to the mixing between the doublet Higgs fields and the singlet Higgs field, the SM-like Higgs boson h may either be the lightest CP-even Higgs boson or the next-to-lightest CP-even Higgs boson, which corresponds to the so-called pull-down case or the push-up case[6], respectively. Although the mass of the SM-like Higgs boson in the nMSSM is quite similar to that in the NMSSM, the Higgs signal is quite different. This is because the peculiarity of the neutralino sector in the nMSSM, where the lightest neutralino $\tilde{\chi}_1^0$ as the lightest supersymmetric particle(LSP) acts as the dark matter candidate, and its mass takes the form[22]

$$m_{\tilde{\chi}_1^0} \simeq \frac{2\mu\lambda^2 v^2}{\mu^2 + \lambda^2 v^2} \frac{\tan\beta}{\tan^2\beta + 1} \quad (13)$$

This expression implies that $\tilde{\chi}_1^0$ must be lighter than about 60 GeV for $\lambda < 0.7$ (perturbativity bound) and $\mu > 100\text{GeV}$ (from lower bound on chargino mass). And $\tilde{\chi}_1^0$ must annihilate by exchanging a resonant light CP-odd Higgs boson to get the correct relic density. For such a light neutralino, the SM-like Higgs boson around 125GeV tends to decay predominantly into light neutralinos or other light Higgs bosons[19].

B. The di-photon Higgs signal

Considering the di-photon signal is of prime importance to searching for Higgs boson near 125 GeV, it is necessary to estimate its signal rate, and we define the normalized production rate as

$$\begin{aligned} R_{\gamma\gamma} &\equiv \sigma_{SUSY}(pp \rightarrow h \rightarrow \gamma\gamma)/\sigma_{SM}(pp \rightarrow h \rightarrow \gamma\gamma) \\ &\simeq [\Gamma(h \rightarrow gg)Br(h \rightarrow \gamma\gamma)]/[\Gamma(h_{SM} \rightarrow gg)Br(h_{SM} \rightarrow \gamma\gamma)] \\ &= [\Gamma(h \rightarrow gg)\Gamma(h \rightarrow \gamma\gamma)]/[\Gamma(h_{SM} \rightarrow gg)\Gamma(h_{SM} \rightarrow \gamma\gamma)] \times \Gamma_{tot}(h_{SM})/\Gamma_{tot}(h) \\ &= C_{hgg}^2 C_{h\gamma\gamma}^2 \times \Gamma_{tot}(h_{SM})/\Gamma_{tot}(h) \end{aligned} \quad (14)$$

where C_{hgg} and $C_{h\gamma\gamma}$ are the couplings of Higgs to gluons and photons in SUSY with respect to their SM values, respectively. In SUSY, the hgg coupling arises mainly from the loops mediated by the third generation quarks and squarks, while the $h\gamma\gamma$ coupling has additional

contributions from loops mediated by W-boson, charged Higgs boson, charginos and the third generation leptons and sleptons. Their decay widths are given by[9]

$$\Gamma(h \rightarrow gg) = \frac{G_F \alpha_s^2 m_h^3}{36\sqrt{2}\pi^3} \left| \frac{3}{4} \sum_q g_{hq} A_{1/2}^h(\tau_q) + \frac{3}{4} \mathcal{A}^{gg} \right|^2 \quad (15)$$

$$\Gamma(h \rightarrow \gamma\gamma) = \frac{G_F \alpha^2 m_h^3}{128\sqrt{2}\pi} \left| \sum_f N_c Q_f^2 g_{hff} A_{1/2}^h(\tau_f) + g_{hWW} A_1^h(\tau_W) + \mathcal{A}^{\gamma\gamma} \right|^2, \quad (16)$$

with $\tau_i = m_h^2/(4m_i^2)$, and

$$\begin{aligned} \mathcal{A}^{gg} &= \sum_i \frac{g_{h\bar{q}_i q_i}}{m_{\bar{q}_i}^2} A_0^h(\tau_{\bar{q}_i}), \\ \mathcal{A}^{\gamma\gamma} &= g_{hH^+H^-} \frac{m_W^2}{m_{H^\pm}^2} A_0^h(\tau_{H^\pm}) + \sum_f \frac{g_{h\bar{f}f}}{m_{\bar{f}}^2} A_0^h(\tau_{\bar{f}}) + \sum_i g_{h\chi_i^+ \chi_i^-} \frac{m_W}{m_{\chi_i}} A_{1/2}^h(\tau_{\chi_i}), \end{aligned} \quad (17)$$

where $m_{\bar{f}}$ and m_{χ_i} are the mass of sfermion and chargino, respectively. In the limit $\tau_i \ll 1$, the asymptotic behaviors of A_i^h are given by

$$A_0^h \rightarrow -\frac{1}{3}, \quad A_{1/2}^h \rightarrow -\frac{4}{3}, \quad A_1^h \rightarrow +7, \quad (18)$$

One can easily learn that the W-boson contribution to $h\gamma\gamma$ is by far dominant, however, for light stau or squarks with large mixing, the $h\gamma\gamma$ coupling can be enhanced. While light squarks with large mixing can suppress the hgg coupling. Therefore, light stau with large mixing may enhance the di-photon signal rate[23], while light squarks with large mixing have little effect on the di-photon signal rate.

III. NUMERICAL RESULTS AND DISCUSSIONS

In our work the Higgs boson mass are calculated by the package NMSSMTools[25], which include the dominant one-loop and leading logarithmic two-loop corrections. Considering the Higgs hints at the LHC, we focus on the Higgs boson mass between 123 GeV and 127 GeV, furthermore, we consider the following constraints:

- (1) The constraints from LHC experiment for the non-standard Higgs boson.
- (2) The constraints from LEP and Tevatron on the masses of the Higgs boson and sparticles, as well as on the neutralino pair productions.

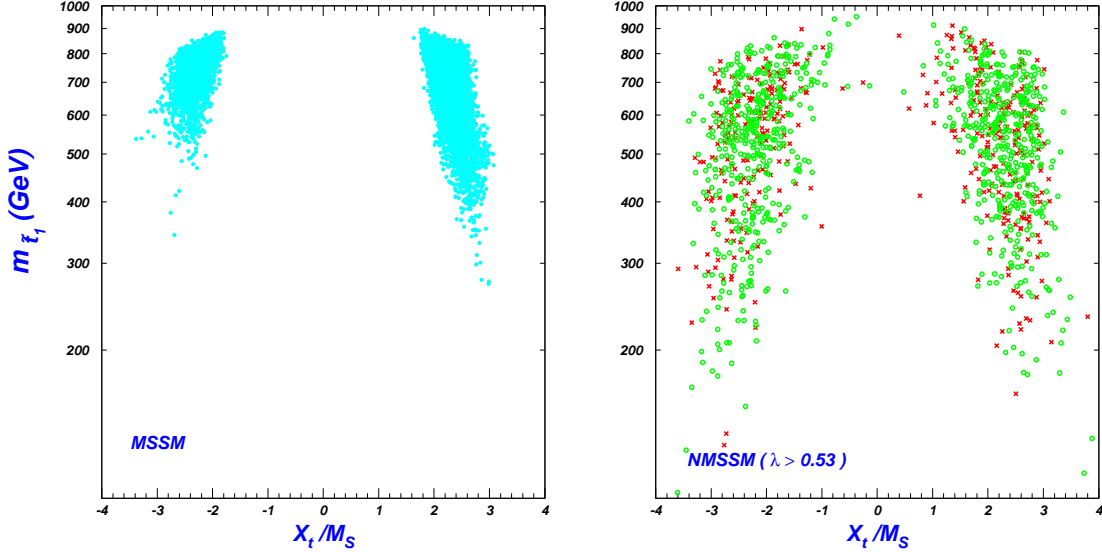


FIG. 1: The scatter plots of the samples in the MSSM and NMSSM (with $\lambda > 0.53$) satisfying various constraints listed in the text (including $123\text{GeV} \leq m_h \leq 127\text{GeV}$), showing the correlation between the mass of the lighter top-squark and X_t/M_S with $M_S \equiv \sqrt{m_{\tilde{t}_1} m_{\tilde{t}_2}}$ and $X_t \equiv A_t - \mu \cot \beta$. In the right panel the circles (green) denote the pull-down case (the lightest Higgs boson being the SM-like Higgs), and the times (red) denote the push-up case (the next-to-lightest Higgs boson being the SM-like Higgs).

- (3) The indirect constraints from B-physics (such as the latest experimental result of $B_s \rightarrow \mu^+ \mu^-$) and from the electroweak precision observables such as M_W , $\sin^2 \theta_{eff}^\ell$ and ρ_ℓ , or their combinations $\epsilon_i (i = 1, 2, 3)$ [26].
- (4) The constraints from the muon $g - 2$: $a_\mu^{exp} - a_\mu^{SM} = (25.5 \pm 8.2) \times 10^{-10}$ [27]. We require SUSY to explain the discrepancy at 2σ level.
- (5) The dark matter constraints from WMAP relic density ($0.1053 < \Omega h^2 < 0.1193$) [28] and the direct detection exclusion limits on the scattering cross section from XENON100 experiment (at 90% C.L.) [29].

Note that most of the above constraints have been encoded in the package NMSSMTools.

Natural supersymmetry are usually characterized by a small superpotential parameter μ , and the third generation squarks with mass $\lesssim 0.5 - 1.5$ TeV[30]. Therefore, we only consider the case with

$$100 \text{ GeV} \leq (M_{Q_3}, M_{U_3}) \leq 1 \text{ TeV}, \quad |A_t| \leq 3 \text{ TeV}. \quad (19)$$

For the case with $\lambda < 0.2$ in the NMSSM, the property of the NMSSM is similar to the case in the MSSM[6]. In order to distinguish the features between MSSM and NMSSM, we only consider the case with $\lambda > m_Z/v \simeq 0.53$ in the NMSSM. We scan over the parameter space of the MSSM and NMSSM under the above experimental constraints and study the property of the Higgs boson for the samples surviving the constraints.

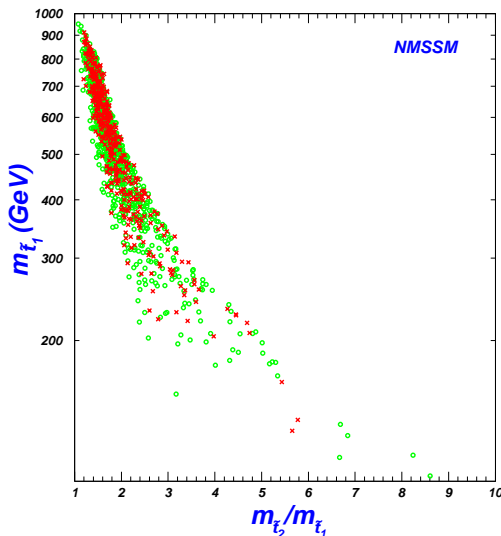


FIG. 2: Same as Fig.1, but only for the NMSSM, showing the correlation between $m_{\tilde{t}_1}$ and the ratio $m_{\tilde{t}_2}/m_{\tilde{t}_1}$.

In Fig.1 we display the surviving samples in the MSSM and NMSSM (with $\lambda > 0.53$), showing the correlation between the lighter top-squark mass and the ratio X_t/M_S with $M_S \equiv \sqrt{m_{\tilde{t}_1} m_{\tilde{t}_2}}$. From the figure we see that for a moderate light \tilde{t}_1 , large X_t is necessary to satisfy $m_h \sim 125$ GeV, and for large $m_{\tilde{t}_1}$, the ratio X_t/M_S decreases. In the MSSM, $|X_t/M_S| > 1.6$ for $m_{\tilde{t}_1} < 1$ TeV, i.e. no-mixing scenario ($X_t = 0$) cannot survive, and the top-squark mass is usually larger than 300 GeV. This implies that a large top-squark mass or a near-maximal stop mixing is necessary to satisfy the Higgs mass near 125 GeV. However, the case is very different in the NMSSM, $X_t \approx 0$ may also survive, and the lighter top-squark mass can be as light as about 100 GeV, which may alleviate the fine-tuning problem and make the NMSSM seems more natural. In the case of light $m_{\tilde{t}_1}$, $|X_t/M_S|$ is usually larger than $\sqrt{6}$, which corresponds to a large splitting between $m_{\tilde{t}_1}$ and $m_{\tilde{t}_2}$, as the Fig.2 shown.

Due to the clean background, the di-photon signal is crucial for searching for the Higgs boson near 125 GeV. As discussed in the Sec.II, the signal rate is relevant with the coupling $C_{h\gamma\gamma}$ and C_{hgg} and the total width of the SM-like Higgs boson. Both the coupling $C_{h\gamma\gamma}$ and

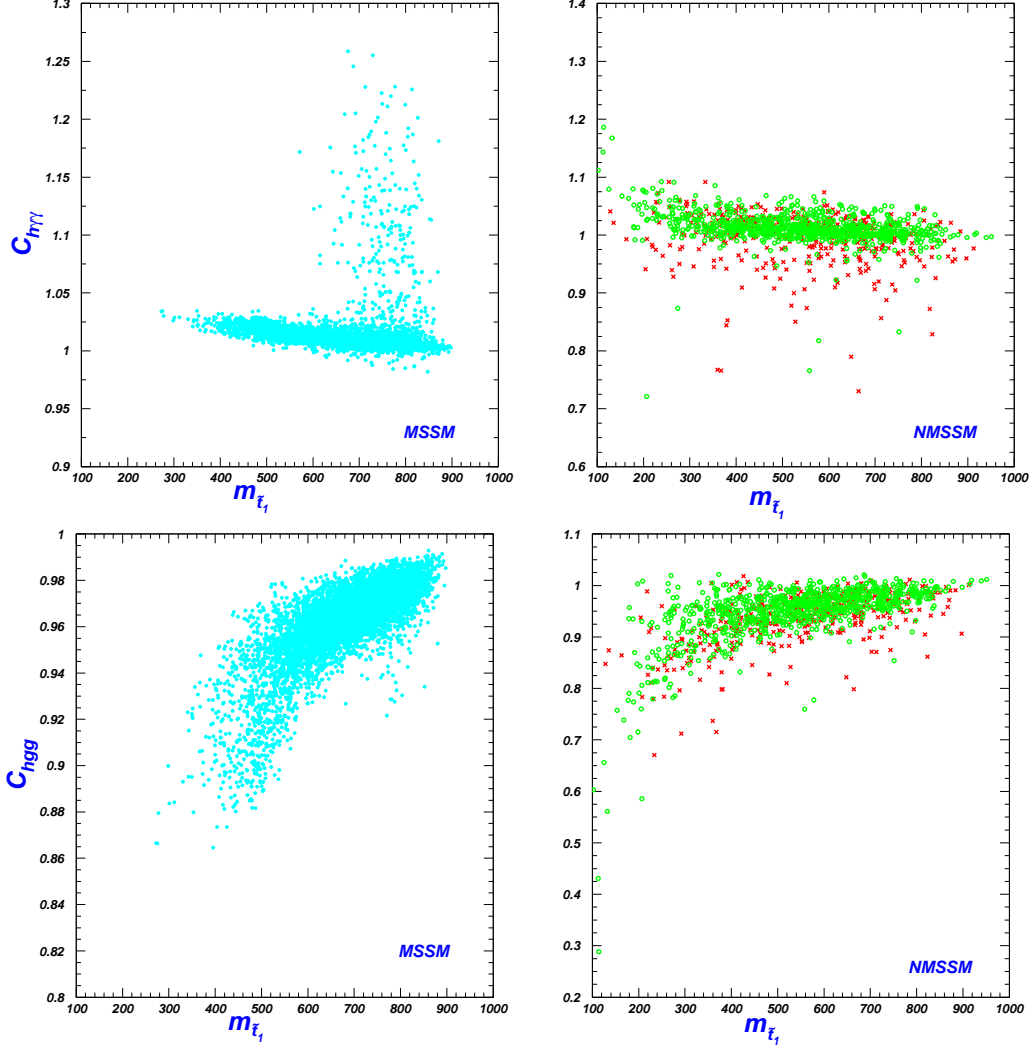


FIG. 3: Same as Fig.1, projected in the planes of $m_{\tilde{t}_1}$ versus the reduced couplings $C_{h\gamma\gamma}$ and C_{hgg} , respectively.

C_{hgg} are affected by the contributions from the squark loops, especially the light top-squark loop, so in the Fig.3 we give the relationship between the lighter top-squark mass and the coupling $C_{h\gamma\gamma}$ and C_{hgg} , respectively. The figure shows that the light $m_{\tilde{t}_1}$ may suppress the coupling C_{hgg} significantly, especially in the NMSSM. While the light top-squark has little effect on the coupling $C_{h\gamma\gamma}$ because there are additional contributions, as the Eq.(15) and Eq.(16) shown. As analyzed in the Sec.II, light stau may enhance the coupling $C_{h\gamma\gamma}$, so in Fig.4 we give the correlation between $m_{\tilde{\tau}_1}$ and the coupling $C_{h\gamma\gamma}$ in the MSSM. The figure clearly shows that the coupling $C_{h\gamma\gamma}$ can enhance to 1.25 for $m_{\tilde{\tau}_1} \sim 100$ GeV. Fig.4 also manifests that the enhancement of the coupling $C_{h\gamma\gamma}$ corresponds to large $\mu \tan \beta$, which leads to large mixing. These results exactly verify the discussions in the Sec.II.

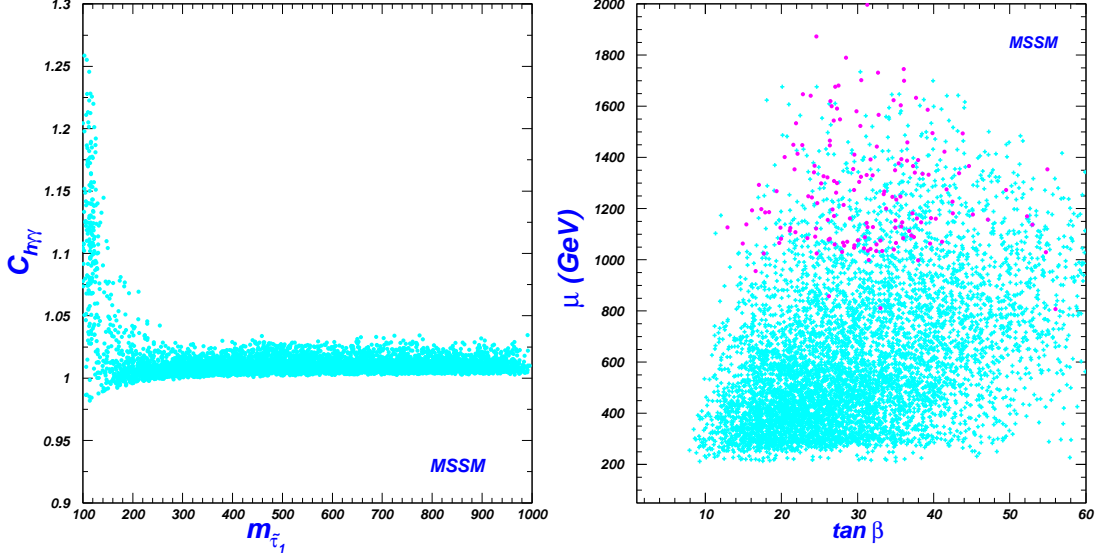


FIG. 4: Same as Fig.1, but only for the MSSM, showing the correlation between $m_{\tilde{\tau}_1}$ and the reduced coupling $C_{h\gamma\gamma}$, μ and $\tan\beta$, respectively. The purple points correspond to $R_{\gamma\gamma} > 1$.

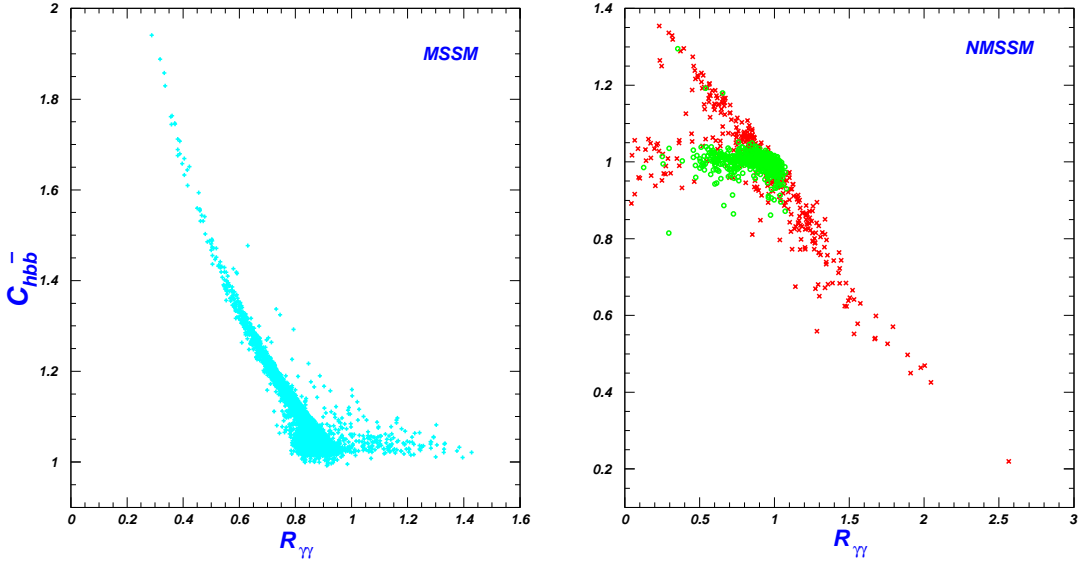


FIG. 5: Same as Fig.1, but showing the dependence of the di-photon signal rate $R_{\gamma\gamma}$ on the effective $hb\bar{b}$ coupling $C_{hb\bar{b}} \equiv C_{hb\bar{b}}^{\text{SUSY}}/C_{hb\bar{b}}^{\text{SM}}$. (taken for Ref.[6])

Since $h \rightarrow b\bar{b}$ is the main decay mode of the light Higgs boson, the total width of the SM-like Higgs boson may be affected by the effective $hb\bar{b}$ coupling $C_{hb\bar{b}}$, as discussed in [17]. Under the effect of the combination $C_{hgg}C_{h\gamma\gamma}/C_{hb\bar{b}}$, the di-photon Higgs signal rate may be either enhanced or suppressed, as shown in Fig.5, which also manifest that for the signal rate larger than 1, the effective $hb\bar{b}$ coupling is enhanced a little in the MSSM, while it is

suppressed significantly in the NMSSM. Therefore, we can conclude that the reason for the enhancement in the signal rate is very different between the MSSM and NMSSM. In the MSSM the enhancement of the signal is mainly due to the enhancement of the coupling $C_{h\gamma\gamma}$, while in the NMSSM it is mainly due to the suppression of the $hb\bar{b}$ coupling.

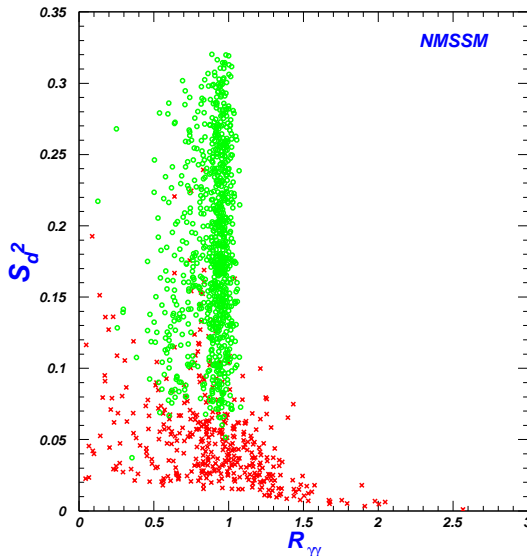


FIG. 6: Same as Fig.2, showing the signal rate R_γ versus S_d^2 with $S_d = C_{hb\bar{b}} \cos \beta$.

Due to the presence of the singlet field in the NMSSM, the doublet component in the SM-like Higgs boson h may be different from the case in the MSSM, which will affect the coupling $hb\bar{b}$, and accordingly affect the total width of h . At the tree-level, $C_{hb\bar{b}} = S_d / \cos \beta$. In Fig.6 we show the dependence of the signal rate R_γ on S_d^2 . Obviously, for the signal rate larger than 1, S_d^2 is usually very small, which leads to large suppression on the reduced coupling $hb\bar{b}$. The figure also shows that the push-up case is more effective to enhance the signal rate than the pull-down case. This is because the push-up case is easier to realize the large mixing between the singlet field and the doublet field[6].

As the case in the NMSSM, nMSSM can also accommodate a 125 GeV SM-like Higgs[17]. However, due to the peculiar property of the lightest neutralino $\tilde{\chi}_1^0$ in the nMSSM[22], the decay mode of the SM-like Higgs is very different from the case in the MSSM and NMSSM. As discussed in the Sec.II, $h \rightarrow \tilde{\chi}_1^0 \tilde{\chi}_1^0$ may be dominant over $h \rightarrow b\bar{b}$ in a major part of parameter space in the nMSSM [17, 31], which induce a severe suppression on the di-photon Higgs signal. Although the Higgs mass can be easily reach to 125 GeV, the di-photon signal is not consistent with the LHC experiment. Therefore, the nMSSM may be excluded by

LHC experiment.

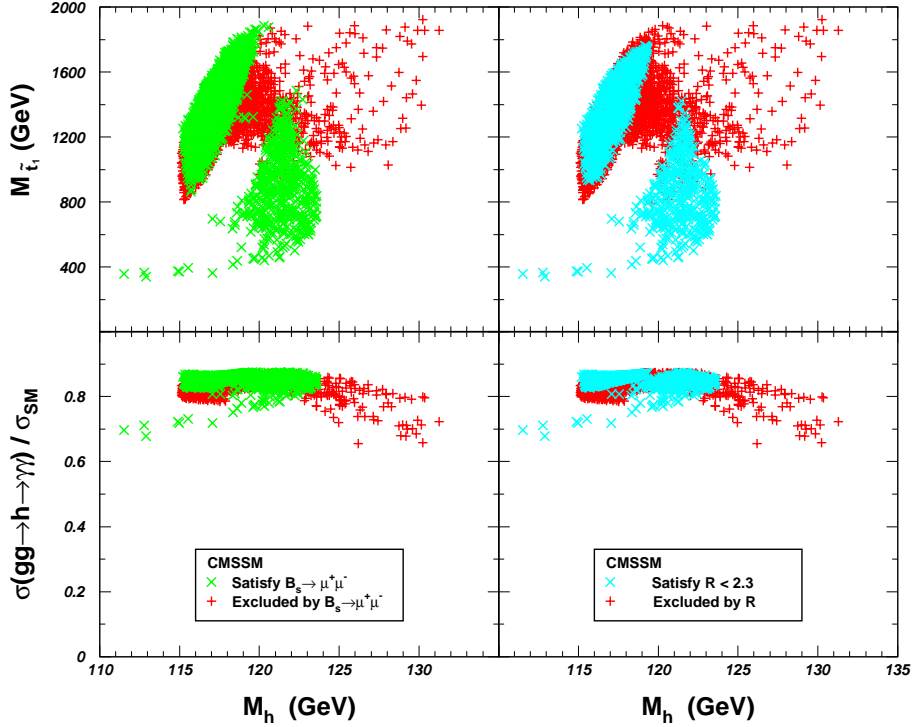


FIG. 7: The scatter plots of the surviving sample in the CMSSM, displayed in the planes of the top-squark mass and the LHC di-photon rate versus the Higgs boson mass. In the left frame, the crosses (red) denote the samples satisfying all the constraints except $B_s \rightarrow \mu^+ \mu^-$, and the times (green) denotes those further satisfying the $Br(B_s \rightarrow \mu^+ \mu^-)$ constraint. In the right frame, the crosses (red) are same as those in the left frame, while the times (sky-blue) denote the samples further satisfying the R constraint.(taken for Ref.[7])

We also considered the SM-like Higgs boson mass and its di-photon signal in the constrained MSSM (including CMSSM and NUHM2) under various experimental constraints, especially the limits from $B_s \rightarrow \mu^+ \mu^-$. Because $Br(B_s \rightarrow \mu^+ \mu^-) \propto \tan^6 \beta / M_A^4$, so it may provide a rather strong constraint on SUSY with large $\tan \beta$. Considering the large theoretical uncertainties for the calculation of $Br(B_s \rightarrow \mu^+ \mu^-)$, we use not only the LHCb data, but also the double ratio of the purely leptonic decays defined as $R \equiv \frac{\eta}{\eta_{SM}}$ with $\eta \equiv \frac{Br(B_s \rightarrow \mu^+ \mu^-) / Br(B_u \rightarrow \tau \nu_\tau)}{Br(D_s \rightarrow \tau \nu_\tau) / Br(D \rightarrow \mu \nu_\mu)}$. The surviving parameter space is plotted in Fig.7 for the CMSSM and Fig.8 for the NUHM2. It shows that both the CMSSM and NUHM2 are hard to realize a 125 GeV SM-like Higgs boson, and also the di-photon Higgs signal is suppressed relative to the SM prediction due to the enhanced $h\bar{b}b$ coupling. Therefore, the constrained MSSM may also be excluded by the LHC experiment.

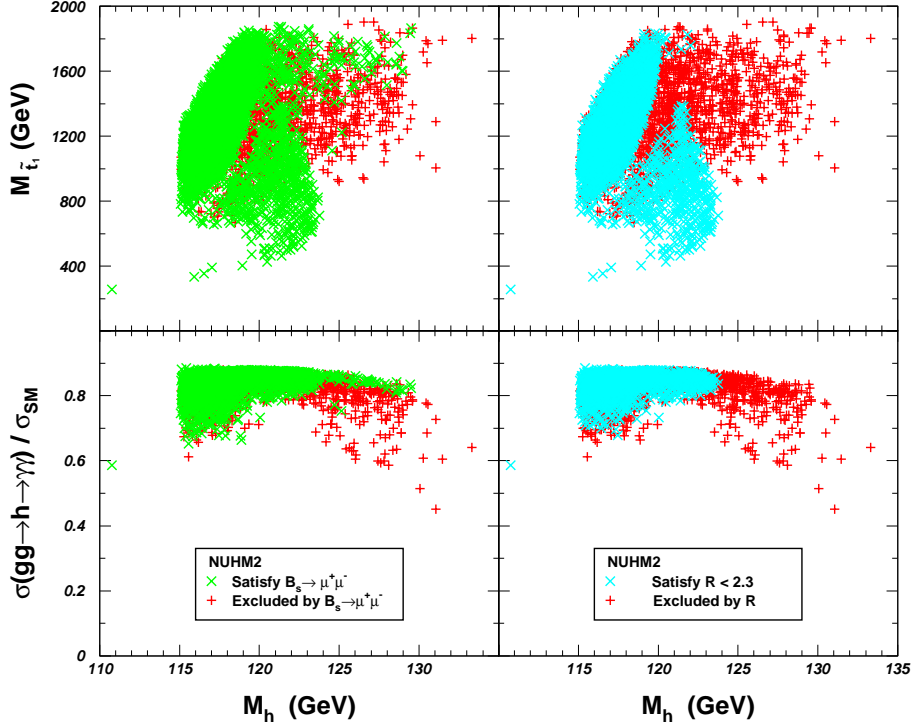


FIG. 8: Same as Fig.7, but for the NUHM2.(taken for Ref.[7])

IV. CONCLUSION

In this work we briefly review our recent studies on a 125 GeV Higgs and its di-photon signal rate in the MSSM, NMSSM, nMSSM and the constrained MSSM. Under the current experimental constraints, we find: (i) the SM-like Higgs can easily reach to 125 GeV in the MSSM, NMSSM and nMSSM, while it is hard to satisfy in the constrained MSSM; (ii) the NMSSM may predict a lighter top-squark than the MSSM, even as light as 100 GeV, which can ameliorate the fine-tuning problem; (iii) the di-photon Higgs signal is suppressed in the nMSSM and the constrained MSSM, but in a tiny corner of the parameter space in the MSSM and NMSSM, it can be enhanced.

Acknowledgement

The work is supported by the Startup Foundation for Doctors of Henan Normal University under contract No.11108.

-
- [1] ATLAS Collaboration, Phys. Lett. B **710**, 49 (2012) [arXiv:1202.1408 [hep-ex]]; Phys. Rev. Lett. **108**, 111803 (2012) [arXiv:1202.1414 [hep-ex]]; Phys. Lett. B **710**, 383 (2012) [arXiv:1202.1415 [hep-ex]].
- [2] CMS Collaboration, JHEP **1204**, 036 (2012) [arXiv:1202.1416 [hep-ex]]; Phys. Lett. B **710**, 403 (2012) [arXiv:1202.1487 [hep-ex]]; Phys. Lett. B **710**, 26 (2012) [arXiv:1202.1488 [hep-ex]]; Phys. Lett. B **710**, 91 (2012) [arXiv:1202.1489 [hep-ex]]; arXiv:1202.1997 [hep-ex]; JHEP **1203**, 040 (2012) [arXiv:1202.3478 [hep-ex]]; JHEP **1203**, 081 (2012) [arXiv:1202.3617 [hep-ex]]; arXiv:1202.4083 [hep-ex]; Phys. Lett. B **710**, 284 (2012) [arXiv:1202.4195 [hep-ex]]; arXiv:1205.2907 [hep-ex].
- [3] D. Carmi, A. Falkowski, E. Kuflik and T. Volansky, arXiv:1202.3144 [hep-ph].
- [4] S. Heinemeyer, O. Stal and G. Weiglein, Phys. Lett. B **710**, 201 (2012); A. Arbey *et al.*, Phys. Lett. B **708**, 162 (2012); L. J. Hall, D. Pinner and J. T. Ruderman, JHEP **1204**, 131 (2012); P. Draper *et al.*, arXiv:1112.3068; A. Arbey, M. Battaglia and F. Mahmoudi, Eur. Phys. J. C **72**, 1906 (2012); O. Buchmueller *et al.*, arXiv:1112.3564; M. Kadastik *et al.*, arXiv:1112.3647; A. Arvanitaki and G. Villadoro, JHEP **1202**, 144 (2012); H. Baer, V. Barger, A. Mustafayev, Phys. Rev. D **85**, 075010 (2012); J. F. Gunion, Y. Jiang and S. Kraml, Phys. Lett. B **710**, 454 (2012); P. Fileviez Perez, Phys. Lett. B **711**, 353 (2012); Z. Kang, J. Li and T. Li, arXiv:1201.5305 [hep-ph]; L. Aparicio, D. G. Cerdeno and L. E. Ibanez, JHEP **1204**, 126 (2012); C. -F. Chang, K. Cheung, Y. -C. Lin and T. -C. Yuan, arXiv:1202.0054 [hep-ph]; J. Ellis and K. A. Olive, arXiv:1202.3262 [hep-ph]; H. Baer, V. Barger and A. Mustafayev, arXiv:1202.4038 [hep-ph]; N. Desai, B. Mukhopadhyaya and S. Niyogi, arXiv:1202.5190 [hep-ph]. F. Boudjema and G. D. La Rochelle, arXiv:1203.3141 [hep-ph]; D. A. Vasquez, G. Belanger, C. Boehm, J. Da Silva, P. Richardson and C. Wymant, arXiv:1203.3446 [hep-ph]; U. Ellwanger and C. Hugonie, arXiv:1203.5048 [hep-ph]; T. Basak and S. Mohanty, arXiv:1204.6592 [hep-ph].

- [5] N. Chen and H. -J. He, JHEP **1204**, 062 (2012); G. Guo, B. Ren and X. G. He, arXiv:1112.3188 [hep-ph]; X. G. He, B. Ren and J. Tandean, arXiv:1112.6364 [hep-ph]; A. Djouadi, *et al.*, Phys. Lett. B **709**, 65 (2012); K. Cheung and T. -C. Yuan, Phys. Rev. Lett. **108**, 141602 (2012); B. Batell, S. Gori and L. -T. Wang, arXiv:1112.5180 [hep-ph]; T. Li, J. A. Maxin, D. V. Nanopoulos and J. W. Walker, Phys. Lett. B **710**, 207 (2012) [arXiv:1112.3024 [hep-ph]].
- [6] J. Cao, Z. Heng, J. M. Yang, Y. Zhang and J. Zhu, JHEP **1203**, 086 (2012) [arXiv:1202.5821 [hep-ph]].
- [7] J. Cao, Z. Heng, D. Li and J. M. Yang, Phys. Lett. B **710**, 665 (2012) [arXiv:1112.4391 [hep-ph]].
- [8] H. E. Haber and G. L. Kane, Phys. Rept. **117**, 75 (1985); J. F. Gunion and H. E. Haber, Nucl. Phys. B **272**, 1 (1986) [Erratum-ibid. B **402**, 567 (1993)].
- [9] A. Djouadi, Phys. Rept. **459**, 1 (2008) [arXiv:hep-ph/0503173].
- [10] For a review, see, e.g., U. Ellwanger, C. Hugonie and A. M. Teixeira, Phys. Rept. **496**, 1 (2010); M. Maniatis, Int. J. Mod. Phys. **A25** (2010) 3505 [arXiv:0906.0777 [hep-ph]]; U. Ellwanger, Eur. Phys. J. C **71**, 1782 (2011) [arXiv:1108.0157 [hep-ph]]; J. R. Ellis, J. F. Gunion, H. E. Haber, L. Roszkowski and F. Zwirner, Phys. Rev. D **39**, 844 (1989).
- [11] For phenomenological studies, see, e.g., J. R. Ellis *et al.*, Phys. Rev. D **39**, 844 (1989); M. Drees, Int. J. Mod. Phys. **A4**, 3635 (1989); S. F. King, P. L. White, Phys. Rev. D **52**, 4183 (1995); B. Ananthanarayan, P.N. Pandita, Phys. Lett. B **353**, 70 (1995); B. A. Dobrescu, K. T. Matchev, JHEP **0009**, 031 (2000); G. Hiller, Phys. Rev. D **70**, 034018 (2004); F. Domingo, U. Ellwanger, JHEP **0712**, 090 (2007); Z. Heng *et al.*, Phys. Rev. D **77**, 095012 (2008); R. N. Hodgkinson, A. Pilaftsis, Phys. Rev. D **76**, 015007 (2007); W. Wang *et al.*, Phys. Lett. B **680**, 167 (2009); J. Cao *et al.*, JHEP **0812**, 006 (2008); Phys. Rev. D **78**, 115001 (2008); J. M. Yang, Int. J. Mod. Phys. D **20**, 1383 (2011).
- [12] A.H. Chamseddine, R. Arnowitt and P. Nath, Phys. Rev. Lett. **49** (1982) 970; R. Barbieri, S. Ferrara and C. Savoy, Phys. Lett. **B119** (1982) 343; L. Hall, J. Lykken and S. Weinberg, Phys. Rev. D **27** (1983) 2359; N. Ohta, Prog. Theor. Phys. **70** (1983) 542.
- [13] J. Ellis, K. Olive and Y. Santoso, Phys. Lett. B **539**, 107 (2002); J. Ellis, T. Falk, K. Olive and Y. Santoso, Nucl. Phys. B **652**, 259 (2003); H. Baer, *et al.*, Phys. Rev. D **71**, 095008 (2005).

- [14] M. S. Carena, J. R. Espinosa, M. Quiros and C. E. M. Wagner, Phys. Lett. B **355**, 209 (1995) [arXiv:hep-ph/9504316]; U. Ellwanger and C. Hugonie, Mod. Phys. Lett. A **22**, 1581 (2007) [arXiv:hep-ph/0612133]; Eur. Phys. J. C **25**, 297 (2002) [arXiv:hep-ph/9909260]; U. Ellwanger, Eur. Phys. J. C **71**, 1782 (2011) [arXiv:1108.0157 [hep-ph]].
- [15] P. H. Chankowski, J. R. Ellis and S. Pokorski, Phys. Lett. B **423**, 327 (1998) [hep-ph/9712234]; R. Barbieri and A. Strumia, Phys. Lett. B **433**, 63 (1998) [hep-ph/9801353]; G. L. Kane and S. F. King, Phys. Lett. B **451**, 113 (1999) [hep-ph/9810374].
- [16] S. Moretti and S. Munir, Eur. Phys. J. C **47**, 791 (2006); K. Hsieh and C. P. Yuan, Phys. Rev. D **78**, 053006 (2008); I. Low and S. Shalgar, JHEP **0904**, 091 (2009); U. Ellwanger, Phys. Lett. B **698**, 293 (2011); JHEP **1203**, 044 (2012).
- [17] J. Cao, Z. Heng, T. Liu, J. M. Yang, Phys. Lett. B **703**, 462 (2011).
- [18] C. Panagiotakopoulos, K. Tamvakis, Phys. Lett. B **446**, 224 (1999); Phys. Lett. B **469**, 145 (1999); C. Panagiotakopoulos, A. Pilaftsis, Phys. Rev. D **63**, 055003 (2001); A. Dedes, *et al.*, Phys. Rev. D **63**, 055009 (2001); A. Menon, *et al.*, Phys. Rev. D **70**, 035005 (2004); V. Barger, *et al.*, Phys. Lett. B **630**, 85 (2005). C. Balazs, *et al.*, JHEP **0706**, 066 (2007).
- [19] J. Cao, H. E. Logan and J. M. Yang, Phys. Rev. D **79**, 091701 (2009); J. Cao, Z. Heng and J. M. Yang, JHEP **1011**, 110 (2010).
- [20] V. Barger *et al.*, Phys. Rev. D **73**, 115010 (2006);
- [21] R. Dermisek and J. F. Gunion, Phys. Rev. Lett. **95**, 041801 (2005); U. Ellwanger, G. Espitalier-Noel and C. Hugonie, JHEP **1109**, 105 (2011).
- [22] J. Cao, Z. Heng and J. M. Yang, JHEP **1011**, 110 (2010) [arXiv:1007.1918 [hep-ph]].
- [23] M. Carena, S. Gori, N. R. Shah and C. E. M. Wagner, JHEP **1203**, 014 (2012).
- [24] S. F. King, M. Muhlleitner and R. Nevzorov, Nucl. Phys. B **860**, 207 (2012);
- [25] U. Ellwanger, J. F. Gunion and C. Hugonie, JHEP **0502**, 066 (2005); U. Ellwanger and C. Hugonie, Comput. Phys. Commun. **175**, 290 (2006).
- [26] G. Altarelli and R. Barbieri, Phys. Lett. B **253**, 161 (1991); M. E. Peskin, T. Takeuchi, Phys. Rev. D **46**, 381 (1992).
- [27] M. Davier *et al.*, Eur. Phys. J. C **66**, 1 (2010).
- [28] J. Dunkley *et al.* [WMAP Collaboration], Astrophys. J. Suppl. **180**, 306 (2009).
- [29] E. Aprile *et al.* [XENON100 Collaboration], Phys. Rev. Lett. **107**, 131302 (2011).
- [30] H. Baer, V. Barger, P. Huang and X. Tata, arXiv:1203.5539 [hep-ph].

[31] J. Cao, Z. Heng, J. M. Yang and J. Zhu, arXiv:1203.0694 [hep-ph].